Analysis of Wind-Induced Thermocline Oscillations of Lake Tanganyika

JAYA NAITHANI[a,*], ERIC DELEERSNIJDER[a] and PIERRE-DENIS PLISNIER[b,c]

[a]*Université catholique de Louvain, Institut d'astronomie et de géophysique Georges Lemaître, Chemin du Cyclotron 2, B-1348 Louvain-La-Neuve, Belgium;* [b]*Royal Museum for Central Africa, Geology and Mineralogy Department, Leuvensesteenweg 13, B-3080 Tervuren, Belgium;* [c]*Facultés Universitaires Notre-Dame de la Paix, Laboratoire d'Ecologie des Eaux Douces, Rue de Bruxelles 61, B-5000 Namur, Belgium*

Abstract. An analysis is presented of the wind-induced thermocline oscillations of Lake Tanganyika, East Africa. The region undergoes a four month dry season and the wet season for the rest of the year. The dry season is characterised by nearly constant high southeasterly winds, while for the rest of the year mild wind blows generally from the northeast. Observations show that the dry season high winds cause tilting of the thermocline, being higher/lower than normal at the southern/northern ends of the lake. The thermocline tries to restabilise itself after the cessation of dry season winds and oscillates for the rest of the year. A non-linear reduced-gravity model is used to study the thermocline oscillations of the lake. The numerical simulations satisfactorily represent the oscillations, their period and amplitude. Different forcing conditions (thermocline depth, wind stress and stability) are used in the model and their effect on the period and amplitude of the oscillations are studied. The amplitude of oscillations ranges from 15 to 45 m, while their period varies from 3 to 4 weeks according to the variation in the model parameters. Wavelet transform is used to study the evolution of periods of oscillations with depth in the time series of observations and along the length of the lake using model simulations. Wavelet spectra presents several dominant modes including the semidiurnal, diurnal, synoptic, intraseasonal variability, besides the modes representing the wind-induced thermocline oscillations.

Key words: continuous wavelet transform, Lake Tanganyika, Morlet wavelets, reduced-gravity model, thermocline oscillations

1. Introduction

Lake Tanganyika is situated in East Africa between four countries, i.e., Congo, Burundi, Tanzania, and Zambia (Figure 1a). It lies between 3°20′ to 8°45′ S and 29°05′ to 31°15′ E. The lake is 650 km long and 50 km wide on average. It is situated at an altitude of about 773 m above sea level. The lake has two basins, with the maximum depth of the northern and southern basins being around 1320 and 1470 m, respectively (Figure 1b). The average depth of the lake is around 570 m. It is the second deepest lake in the world. It plays an important role in the economy and food source of the neighbouring countries. The water temperature in

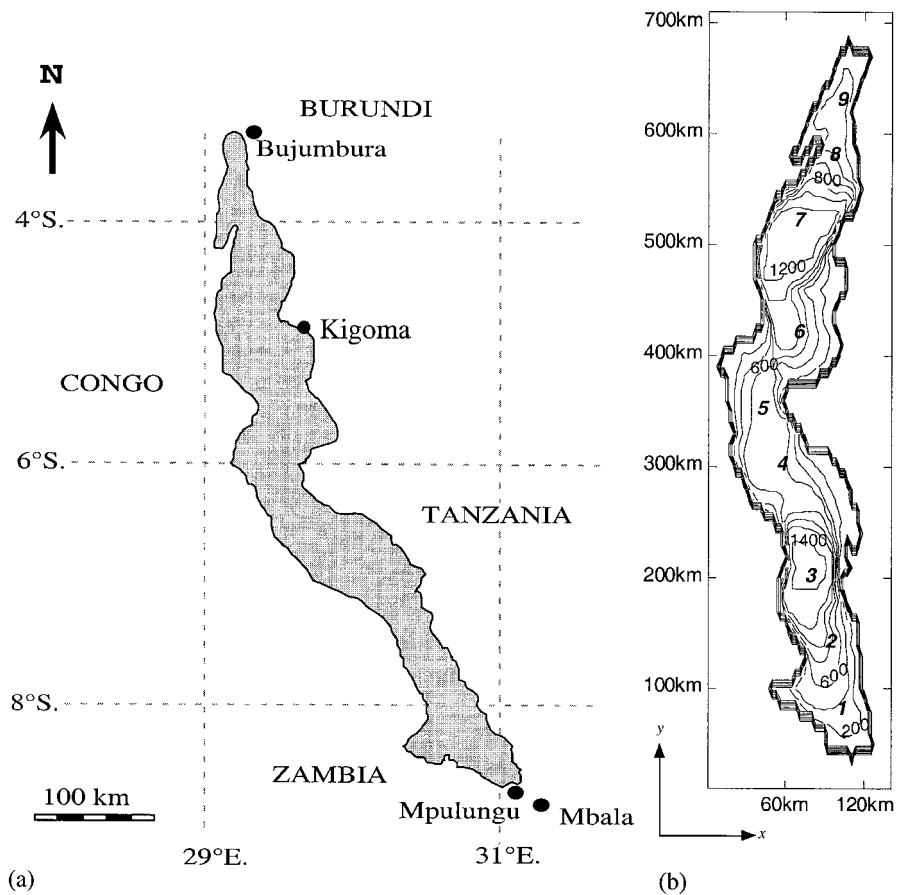*Corresponding author, E-mail: naithani@astr.ucl.ae.be

Figure 1. Map of Lake Tanganyika (a) and the Lake bathymetry (b) as presented in the model domain (contours are drawn at 200 m interval).

the lake varies from 24–28 °C in the surface layer to around 23.5 °C in the bottom layer. The lake is characterised by a permanent anoxic hypolimnion below about 100 m in the north and 200 m in the south. Thermal stratification in the lake is well marked and varies seasonally above the permanent hypolimnion [1].

Due to its close proximity to the equator, the solar radiation over the region surrounding the lake varies very little in the year. The main seasons around the lake are a four-month long 'dry season', characterised by cooler dry weather and fairly constant southeasterly (trade) winds from around May to September, and a 'wet season' during the rest of the year, during which the winds are weaker and mainly northeasterly [1]. Wind speed during the dry season reaches 7–9 m/sec with gusts of 10–12 m/sec. During the high winds of the dry season there is a loss of heat from the lake by evaporation. The wind stress pushes the warmer surface water away from the southern end of the lake towards the northern end and an upwelling occurs to replace the loss of water at the south. The epilimnion water accumulates

at the north and is pulled downwards by gravity. A counter-current flows back near the thermocline to the south in the direction opposite to the prevailing winds. The thermocline gets tilted downward towards the north and totally disappears in the south. The stratification totally breaks down at the southern extremity and becomes very weak throughout the south basin, while in the north the stratification and the thermocline persist throughout the dry season. The nutrient rich water upwelled at the south reaches the northern end of the lake 2–3 weeks after the dry season wind stops [1]. The time taken by this water to mix well over the length of the lake to the thermocline depth is much longer than the dry season. This is due to the vertical mixing counteracting the horizontal advection [2]. This 2–3 weeks time is same as the time taken by an internal surge, to propogate the length of the lake from the north towards the south after the SE wind stops at the end of the dry season. The displaced layers slide over each other to redistribute into a new equilibrium. The oscillations give rise to internal instability and waves with wavelengths of the order of lake dimensions. These progressive waves get reflected at the Lake boundaries and gradually transform into standing wave patterns [1], called internal seiches. From September–November, heating occurs in the lake which reestablishes the stratification and thermocline tends to stabilise. By December the thermocline reaches the level (around 50 m) at which it remains during the wet season and oscillates. These oscillations persist throughout the wet season until the following seasonal onset of southeasterly winds [1, 3].

Internal seiches help in the mixing of nutrient rich bottom water because of much greater water movements associated with them. The resulting currents rythmically flow back and forth in opposing directions and are the major water movements of the lake in an otherwise stratified lake. These currents cause vertical and horizontal distribution of heat, dissolved substances and nutrients from the bottom layer. This significantly alters the distribution and productivity of phytoplankton and fishes [1, 4]. The wind-driven upwelling of anoxic water, which may be strong enough to result initially in fish kills due to anoxia in the south, causes phytoplankton blooms due to the increase of the nutrients rich deep water in the photic layers of water. The phytoplankton blooms soon result in an increase in the production of fishes. In the absence of sufficiently strong wind stress and the resulting seiches, the chances of the bottom water mixing with the surface water over the length of the lake would be difficult. Due to its large size, strong vertical gradient in nutrients and sensitivity to the southeasterly winds chanelled through its S–N axis, the lake is sensitive to the variability in the climate. Over recent years, it has been observed that the lake hydrodynamics exhibits a variability according to changing climate and events like teleconnections of El Nino – Southern Oscillation (ENSO) affecting East Africa [5, 6]. For instance, correlations have been found between ENSO and pelagic fish catches [5]. During ENSO year, when the temperatures are rather high, the thermocline is shallow and the winds are low, the resulting windstress is not sufficient to cause significant mixing of the nutrient rich bottom water.

The resulting phytoplankton bloom and fish production are not sufficient, affecting the economy and food stock of the neighbouring countries.

Understanding the lake hydrodynamics and its variability is important for the management of its resources. In this respect, numerical modelling is an invaluable tool. A numerical model, once validated, can simulate the actual conditions in the lake even in the absence of lengthy, time consuming and hard to obtain observations. Collecting field data is difficult over lake Tanganyika, due to its vast length and the 4 developing countries sharing it. Our objective is to build a three-dimensional model of the lake hydrodynamics and couple it to an ecological model. The first stage of the undertaking is concerned with the study of the tilting of the thermocline during the dry season and the large-amplitude oscillations of the thermocline (internal seiches) induced by wind stress. This paper presents an analysis of the thermocline oscillations using observations and simulations by means of a two-dimensional reduced-gravity model. Section 2 discusses the observed time series of temperature at various depths and Section 3 presents the continuous wavelet transform used to study the evolution of various modes of oscillations present in the time series of temperature at various depths near Mpulungu. Description of the reduced-gravity model to study the thermocline displacement is given in Section 4. Section 5 discusses the model simulations of the downward displacement of the thermocline and the periods of oscillations, whereas, the sensitivity to various model parameters is studied in Section 6. Finally, concluding remarks are presented in Section 7.

2. Observations

Figure 2a shows the time series of daily-averaged wind speed and direction for the period from 1 April 1993 to 31 March 1994 for Mpulungu, the southernmost site marked on Figure 1a. The data were collected during the FAO/FINNIDA project. The data were recorded at every hour. The figure shows high winds for the period of May to early September (dry season) from the southeast. Average wind during the dry season was around 5 m/s, while wind gusts as high as 12 m/sec were also present. During the wet season the winds were low and variable. Figure 2b depicts the temperature distribution with depth and time for the data collected from the buoy moored near Mpulungu for the same period. An Anderaa thermistor chain was anchored at 320 m depth, 30 km north of Mpulungu. The thermistors were placed at 11 depths (1, 5, 30, 50, 70, 90, 110, 150, 200, 250 and 300 m). The precision of the instrument is $0.01\,°C$. Temperature isotherms show lower temperatures for the whole depth during the dry season. With the commencement of the dry season winds around May, the temperature of upper layers of the Lake started decreasing. The lower temperatures during the dry season are initially due to the combined influence of evaporative cooling, convective mixing and wind-generated vertical mixing in the upper layers [1]. The lake gets well mixed in the upper 200 m. According to Coulter and Spigel [1] loss of heat from the Lake is mainly caused by
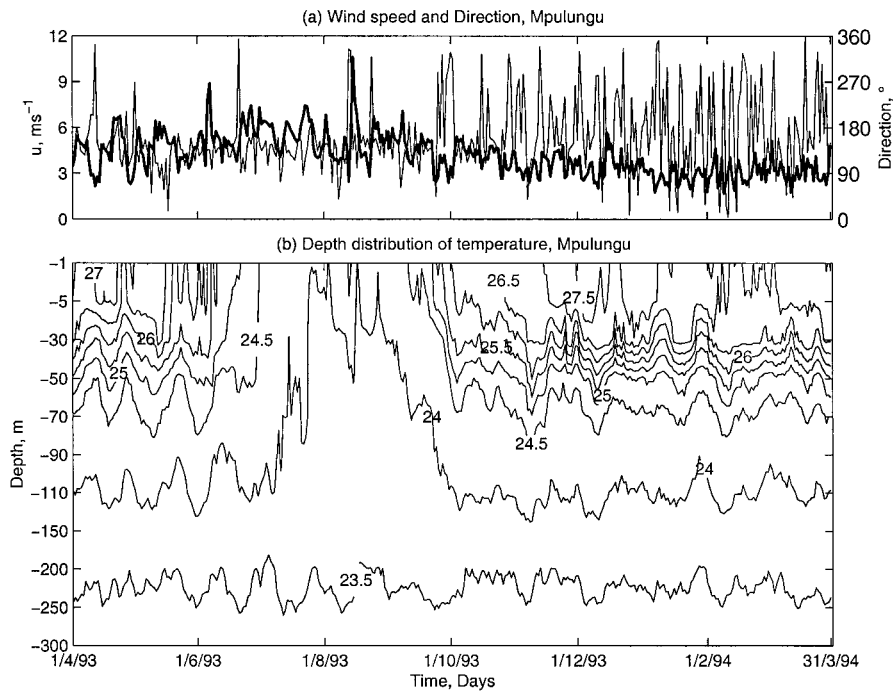
Figure 2. Time series of (a) daily averaged wind speed (thick line) and direction (thin line) and (b) temperature distribution with depth of the Lake Tanganyika for the period 1993–1994 at Mpulungu.

evaporative cooling by the south wind. Seasonal evaporative cooling by the south wind over approximately the same period also occurs in Lake Victoria [7] and in Lake Malawi [8]. In both lakes evaporation rates seem to be higher in their southern ends [8, 9]. Soon, as the surface water is pushed towards the north by continuously high SE winds, an upwelling from below occurs at the southern end to replace the loss of water. The upwelling is easily seen in the decreased pH of the surface water during dry season (not shown here). The pH of bottom water is lower than that of the surface water, where the photosynthesis consumes much of the carbon dioxide. This upwelled cold bottom water decreases the vertical temperature gradient between various layers in the south and at the same time further increases the horizontal temperature gradient between the south and the north ends. By end of June the temperature gradient between the layers near the surface and down to the depth of 150 m was reduced to less than 0.5 °C. The temperature of various layers started readjusting to the normal magnitude at the end of September. The temperature near the surface was around 24 °C during much of the dry season and around 27 °C for the rest of the year, while it was around 23.5 °C below 200 m throughout the year. The figure depicts oscillations for the whole year down to a depth of 300 m.
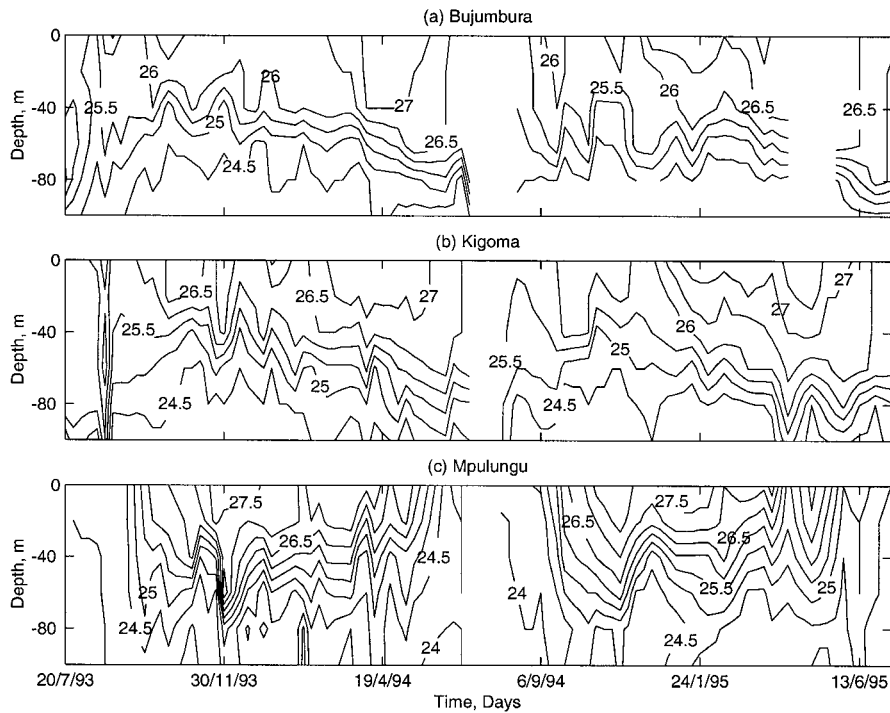
Figure 3. Temperature distribution with depth for (a) Bujumbura, (b) Kigoma and (c) Mpulungu for the years 1993–1995.

To see the temperature variation with depth along the length of the Lake, the dataset collected every week at three sites of the lake, Mpulungu, Kigoma and Bujumbura, from July 1993 until June 1995 are used. These sites are marked on Figure 1a. Temperatures were recorded at every 20 m down to the depth of 100 m. The measurements were performed using a Yellow Spring Instrument. Temperature precision of this instrument is 0.1 °C. Figure 3 shows the temperature isotherms for the three sites. The figure shows the thermocline being lower at the northern sites (Figures 3a, b) and shallower or absent in the southern site (Figure 3c) during the dry season (approximately in the middle and at the two ends of the plots). The tilting of the thermocline is, as explained in the introduction, due to the southeast winds which push the water towards the north. The vertical temperature difference in the south during the dry season is reduced to 0.5 °C, while in the north it continues to persist and maintains the stratification. However, the effect of evaporative cooling, convective mixing and wind generated mixing in the dry season can also be seen in decreasing the temperature of the upper layers at northern sites. During the dry season upwelling is seen at Mpulungu. The (differential) evaporative cooling throughout the Lake, upwelling at the southern end and horizontal advection of the near surface layer water from the southern end to the north modify the horizontal temperature gradient in the dry season. Two to three weeks after the

dry season wind stops and the thermocline at the northern sites rises. This abrupt rise of the thermocline in the northern sites, immediately after the south wind stops, might be called a secondary upwelling. These figures again show the oscillations throughout the year at all of the three stations. The oscillations are also seen in the dry season.

3. Continuous Wavelet Transform Spectra

In order to determine the periods of oscillations present in various layers of the Lake, wavelet transform (WT) of the time series given in Figure 2b is performed. Wavelet transform is used instead of the classical Fourier transform, since it allows the visualisation of the time evolution of various scales present in the multiscale time series. WT gives the time-frequency representation of the multiscale time series. This includes the variation of intensity of a particular scale with time. Continuous Morlet wavelets are used, since they best represent the presence of various scales localised in frequency and time continuously. A Morlet wavelet is defined as:

$$\Psi(t) = \pi^{-1/4} \exp(-i\omega_\circ t) \exp\left[\frac{-t^2}{2}\right], \tag{1}$$

where t is the time and $\omega_\circ$ is a nondimensional center frequency defined so that the second maximum of real part of the function is half of the first one, i.e., $\omega_{\circ(t=0)} \geq \pi/\sqrt{(2/\ln 2)}$. In order to avoid extensive computational time the WT is performed in the Fourier space. Fourier transform (FT) of Morlet wavelet is approximated as:

$$\hat{\Psi}(\omega) = \pi^{-1/4} \exp\left[\frac{-(\omega_\circ - \omega)^2}{2}\right], \tag{2}$$

where $\omega = 2\pi n/N, n = 0, 1,...n$, N is the length of the time series. The WT of the time series is the convolution of the time series with the scaled and translated form of the mother wavelet (in our case Morlet wavelet). Thus we define the scaled Morlet wavelet in Fourier space as:

$$\hat{\Psi}_{a,0}(\omega) = \sqrt{a}\,\pi^{-1/4} \exp\left[\frac{-(\omega_\circ - a\omega)^2}{2}\right]. \tag{3}$$

The wavelet scale can be related to the Fourier period. For Morlet wavelet this relation is given as [10]:

$$a = \frac{1}{4\pi}\left[\omega_\circ + \left(2 + \omega_\circ^2\right)^{1/2}\right]\lambda. \tag{4}$$

To reduce further machine time consumption, the wavelets are divided into frequency bands or octaves. The continuous transform is carried out on the discrete
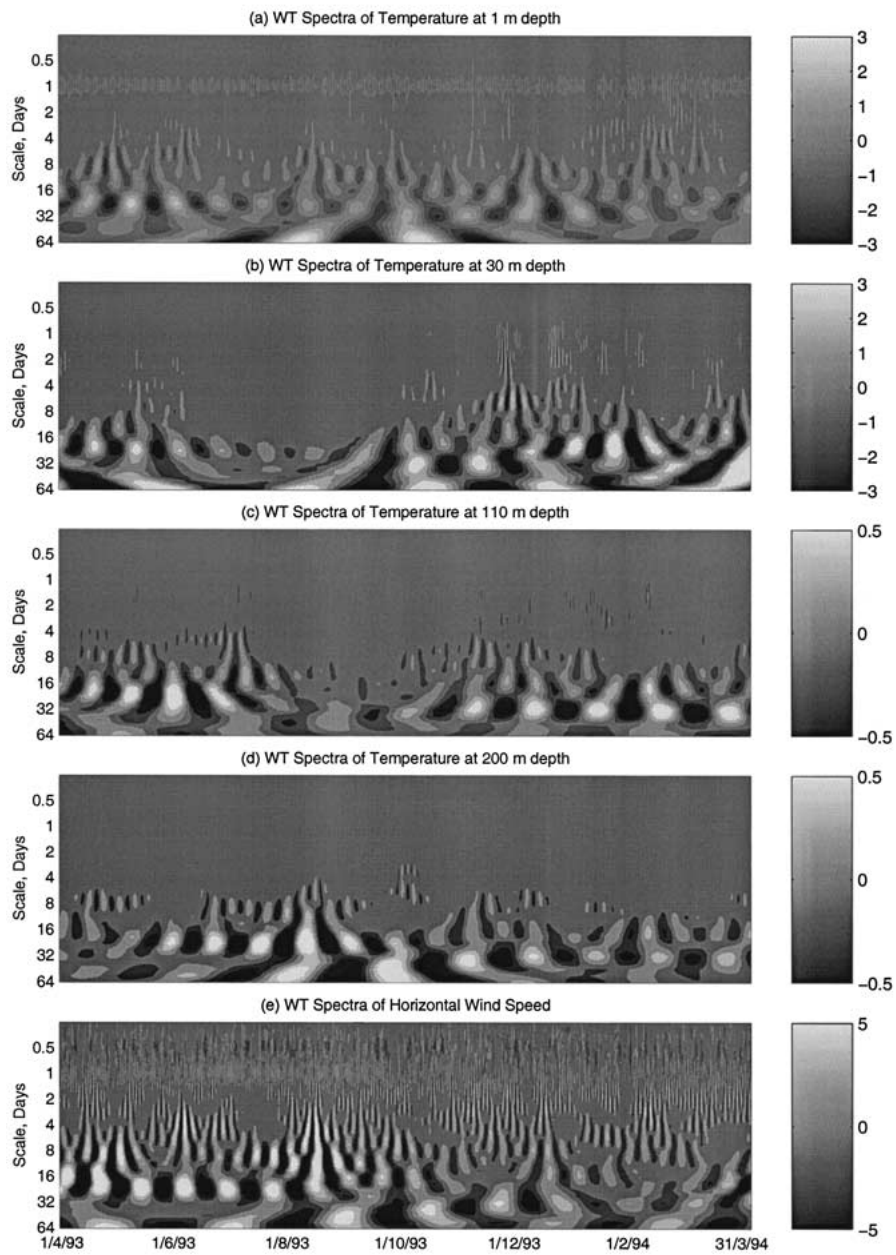
Figure 4. Time-scale representation of the real part of the continuous Morlet wavelet coefficients based on three hourly data for (a-d) water temperature at the depths of 1, 30, 110 and 200 m and (e) wind speed, respectively near mpulungu for April 1993 to March 1994.

sets of wavelets at dyadic scales, defined as $a = a_\circ 2^m$, where m is an integer and $a_\circ$ is the minimum scale.

Figure 4 presents the real part of the complex Morlet wavelet coefficients of the time series of temperature at depths of 1, 30, 110 and 200 m, respectively (Figures 4a–d) at Mpulungu. The real part of the wavelet coefficients gives an insight into the energy density and the phase. The shading density represents the intensity of the signal in the wavelet domain. This figure shows several dominant scales including the semidiurnal, diurnal, synoptic, and intraseasonal variability, besides the modes representing the wind-induced thermocline oscillations. The evolution of various scales with time of the year and with depth is clearly visible. WT of the time series of temperature at 1 m depth (Figure 4a) show peaks around 11, 22 and 33 days along with the diurnal peaks. The WT spectra of temperature at depths of 30, 110 and 200 m, respectively (Figures 4b–d) show two main peaks at around 22 and 33 days. The 22 day peak show maximum intensity during the dry season, while the 33 day peak is more prominent in the wet season after the cessation of dry season winds. It is interesting to note that these two oscillations are observed down to the depth of 200 m, however with decreasing intensity and slightly increasing periods. The maxima in intensity of the 22 day peak, which is more to the beginning of the dry season (around May) near the surface shifts more towards the end of the dry season (around August) with depth. WT spectra of temperature at 1 and 30 m depths show synoptic variability around 3, 6 and 12 days more prominent in the wet season. The 6 and 12 day scale is also seen in the lower depths.

The wavelet spectra of the time series of wind at Mpulungu site is also performed. This is done since the thermocline oscillations are caused by wind forcing acting over the lake surface. Figure 4e shows the real part of the continuous wavelet coefficients of the 3 hourly averaged horizontal wind at Mpulungu for the same period as in Figure 2a. The wavelet transform spectra of wind shows semidiurnal and diurnal variation which are more prominent in the dry season. The wind spectra also show peaks around 11, 22 and 33 days. The diurnal variability and the 22 day peak are present in the dry season, while the 33 day peak is visible in the wet season. The salient features in the wind spectra is similar to those of the spectra of temperature in the water. From the above figure (Figure 4e) we can assume that the spectra of wind near the water surface could be used as an indicator of the primary modes of oscillation present within the Lake.

4. Model Description

Internal oscillations are rather well reproduced by a two-dimensional reduced-gravity model, which is developed and used for the purpose of the present study. In using a reduced-gravity model, one assumes that the density stratification is much more important in determining the internal oscillations than the underlying bottom topography. In lake Tanganyika, it is appropriate to have recourse to such a model since, as explained above, stratification is present all year round and the
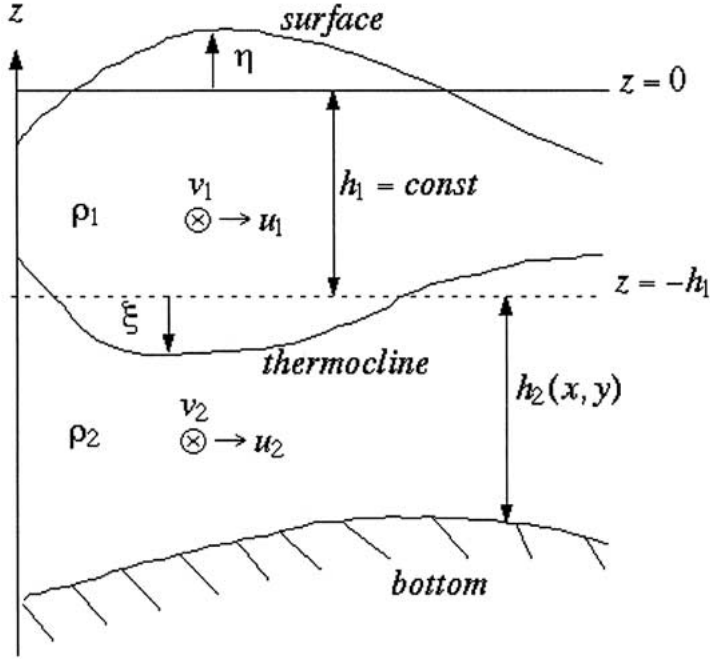
Figure 5. The main parameters and variable of a two-layer model, which upon assuming that $h_2 >> h_1$, gives rise to a reduced-gravity model.

depth of the surface mixed layer is generally much smaller than the thickness of the hypolimnion. The usefulness of a reduced-gravity model in explaining seasonal and interannual variability in vertically integrated quantities in the upper layer in response to wind forcing has been demonstrated by Busalacchi and O'Brien [11, 12]. This type of model has also proved to be useful in explaining many observed features in the upper layer of the ocean [13, 14]. Young *et al.* [15] used this model to study the local and nonlocal response of Conception Bay to wind-forcing, while Inoue and Welsh [16] have used this model to study the seasonal variability in the wind-driven upper-layer circulation. Recently, Handoh *et al.* [17] have used this type of model to study the primary productivity in the tropical open ocean.

The model domain is presented in Figure 1b. In the model domain, x-axis is along the width of the lake while the y-axis is along the length of the lake. The model consists of two layers of different densities. The surface layer is considered to be of finite depth and the bottom layer of infinite depth, which is a fairly good approximation as the average depth of the water column is around 600 m, while the depth of the epilimnion is of the order of 50 m. Figure 5 presents the conceptual view of the two-layer model giving rise to the reduced-gravity model. The governing equations for the model top layer are:

$$\frac{\partial \xi}{\partial t} + \frac{\partial}{\partial x}(H_1 u_1) + \frac{\partial}{\partial y}(H_1 v_1) = 0 \tag{5}$$

$$\frac{\partial}{\partial t}(H_1 u_1) + \frac{\partial}{\partial x}(H_1 u_1 u_1) + \frac{\partial}{\partial y}(H_1 v_1 u_1) - f H_1 v_1 =$$
$$-\varepsilon g H_1 \frac{\partial \xi}{\partial x} + \frac{\partial}{\partial x}\left(k_x H_1 \frac{\partial u_1}{\partial x}\right) + \frac{\partial}{\partial y}\left(k_y H_1 \frac{\partial u_1}{\partial y}\right) + \frac{\tau_w^x}{\rho_0} - \frac{\tau_p^x}{\rho_0} \tag{6}$$

$$\frac{\partial}{\partial t}(H_1 v_1) + \frac{\partial}{\partial x}(H_1 u_1 v_1) + \frac{\partial}{\partial y}(H_1 v_1 v_1) + f H_1 u_1 =$$
$$-\varepsilon g H_1 \frac{\partial \xi}{\partial y} + \frac{\partial}{\partial x}\left(k_x H_1 \frac{\partial v_1}{\partial x}\right) + \frac{\partial}{\partial y}\left(k_y H_1 \frac{\partial v_1}{\partial y}\right) + \frac{\tau_w^y}{\rho_0} - \frac{\tau_p^y}{\rho_0} \tag{7}$$

$$H_1 = h_1 + \eta + \xi \approx h_1 + \xi, \tag{8}$$

where ξ is the downward displacement of the interface between the two layers or the thermocline, u_1 and v_1 are the depth integrated velocity components in the surface layer in the x and y directions, f is the Coriolis parameter, h_1 is the depth of the undisturbed surface layer or the pycnocline depth, εg is the reduced-gravity, g is the acceleration due to gravity, $\varepsilon = \frac{\rho_2 - \rho_1}{\rho_2} \approx 6.3 * 10^{-4} - 9.06 * 10^{-4}$, ρ_1 and ρ_2 are the density of the surface and the bottom layers, k_x and k_y are the eddy viscosities in the two directions, τ_w^x and τ_w^y are the surface wind stresses in x and y directions, while τ_p^x and τ_p^y are the pycnocline or bottom stress in x and y directions respectively, which are not considered in the model. In certain model runs, the upward displacement of the thermocline can be equivalent to the unperturbed depth of the thermocline. To prevent the thermocline from outcropping, an elementary wetting-drying algorithm [18] is implemented, consisting in setting to zero the water fluxes crossing the boundaries of every grid box in which the actual water column depth would become – after one time step – smaller than a critical value, which is taken to be $H_{1min} = 5$ m herein. It is noted that for the model parameters and the wind forcing used in this study, the model interface never becomes shallower than H_{1min}. The thermocline outcrops only for the wind forcing around and greater than 7 ms^{-1} discussed in section 6.

Equations (5–7) are discretised on Arakawa's C grid. The model uses the forward-backward time stepping. Model is initialised with $u_1 = v_1 = \xi = 0$. In the model, an idealised wind forcing is applied, with constant southeasterly winds during the dry season and no wind stress during the rest of the year. The spatially uniform wind stress along the whole length of the lake is provided at the beginning of the fifth month. The wind stress is increased linearly from zero to its maximum value over ten days. The wind stress remains at this maximum value for four months of the dry season and is relaxed back to zero within one day. The four month long wind forcing used is representative of the dry season southeasterly winds. The lake is represented with a rectangular Cartesian grid with $\Delta x = 3$ km and $\Delta y = 10$ km. The time step is 5 min. The model is run for 5 years and the last year of simulations are analysed.
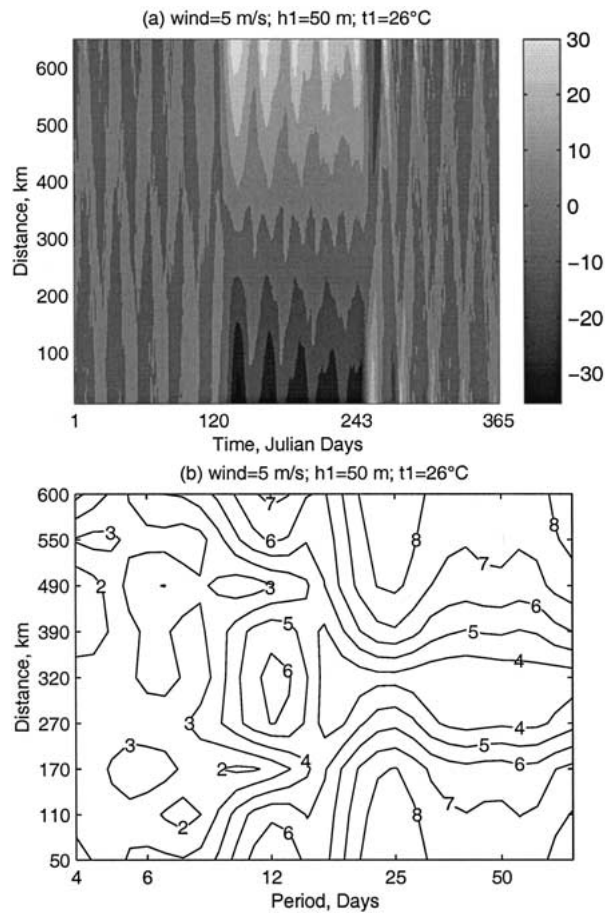
Figure 6. Width-averaged downward displacement of the thermocline in meter as a function of time and the length of the lake (a) and (b) the logarithm of the time-averaged wavelet spectra of the downward displacement of thermocline for the 9 points along the length of the Lake from the southern end, plotted as a function of time and distance. These 9 points are marked on Figure 1b.

5. Model Control Run Simulations

Figure 6a presents the width-averaged downward displacement of the thermocline for a surface layer unperturbed depth of 50 m, dry season southeasterly winds of 5 m/s and temperatures of the surface and the bottom layers at 26 and 23.5 °C, respectively. The figure shows tilting of the thermocline towards the north as the wind stress is applied on the 120th day of each year, while at the southern end, it becomes shallower. The shallowing at the south and the tilting at the north in the dry season is not continuous, but shows oscillations of about 24 days. The amplitude of these internal oscillations slowly decrease due to frictional damping throughout the length of the wet season from August/September to March/April,

after which the stress is applied and the whole process begins once again. The model control run simulates the period of oscillations which is similar to the one presented by the observations, in spite of being forced by constant winds at the dry season.

In order to see if the model simulates other modes of oscillations besides the 24-day fundamental mode depicted in Figure 6a, the downward displacement of the thermocline at 9 points along the length of the lake are further analysed. These 9 points are marked on Figure 1b. The time series at the nine points are analysed using the wavelet transform spectra. The WT spectra of the individual time series for the nine coordinate positions show the presence of 12-and 24-day peaks. The WT spectra also depict a 6-day period being prominent from the middle of the dry season to the year end and is of less intensity in the smaller months of the year and first half of the dry season. All the three modes of oscillations seem to start from the dry season, persist throughout the year and decay towards the beginning of the next dry season. Figure 6b shows the 2-dimensional time-mean wavelet spectra of the thermocline displacement. In the figure, the abscissa is the time in Julian days and the ordinate is the distance in km of the 9 points from the southernmost end of the lake. The figure shows various scales of motion around 6, 12 and 24 days. The 24-day peak being the prominent mode at the northern and the southern proximities of the Lake and is of less intensity at the centre of the Lake. The 12-day peak is prominent around the centre of the lake and at the extreme ends. The presence of various peaks in model simulations are in agreement with various scales of motion observed in the time series of temperature at various depths. We see that besides the fundamental mode of oscillation, both in the observations and model simulation, there are several other free modes of the longitudinal oscillations, which are basically the integer divisions of the fundamental mode.

6. Model Sensitivity Tests

The model control run simulated the oscillations period and amplitude similar to those presented in the observations. This established the credibility of the numerical model and therefore, we simulated further the oscillations for various atmospheric conditions for which the realtime observations are not available, considering them representing the actual oscillations likewise. Sensitivity tests were performed with the model to study the effects of increasing wind stress, thermocline depth and stratification or density of the epilimnion on the amplitude and period of thermocline oscillations. Figure 7 presents the composite of all the tests. From these tests it is inferred that increasing the stratification by 0.5 °C decreases the periods of oscillations at the same time decreasing their amplitude (Figures 7a, b), increasing the thermocline depth also decreases the amplitude of oscillations and their period (Figures 7c, d). Increasing the wind stress and stratification, increases the amplitude of oscillations and decreases the period slightly (Figures 7e, f). It is seen that the model interface or the thermocline touches the
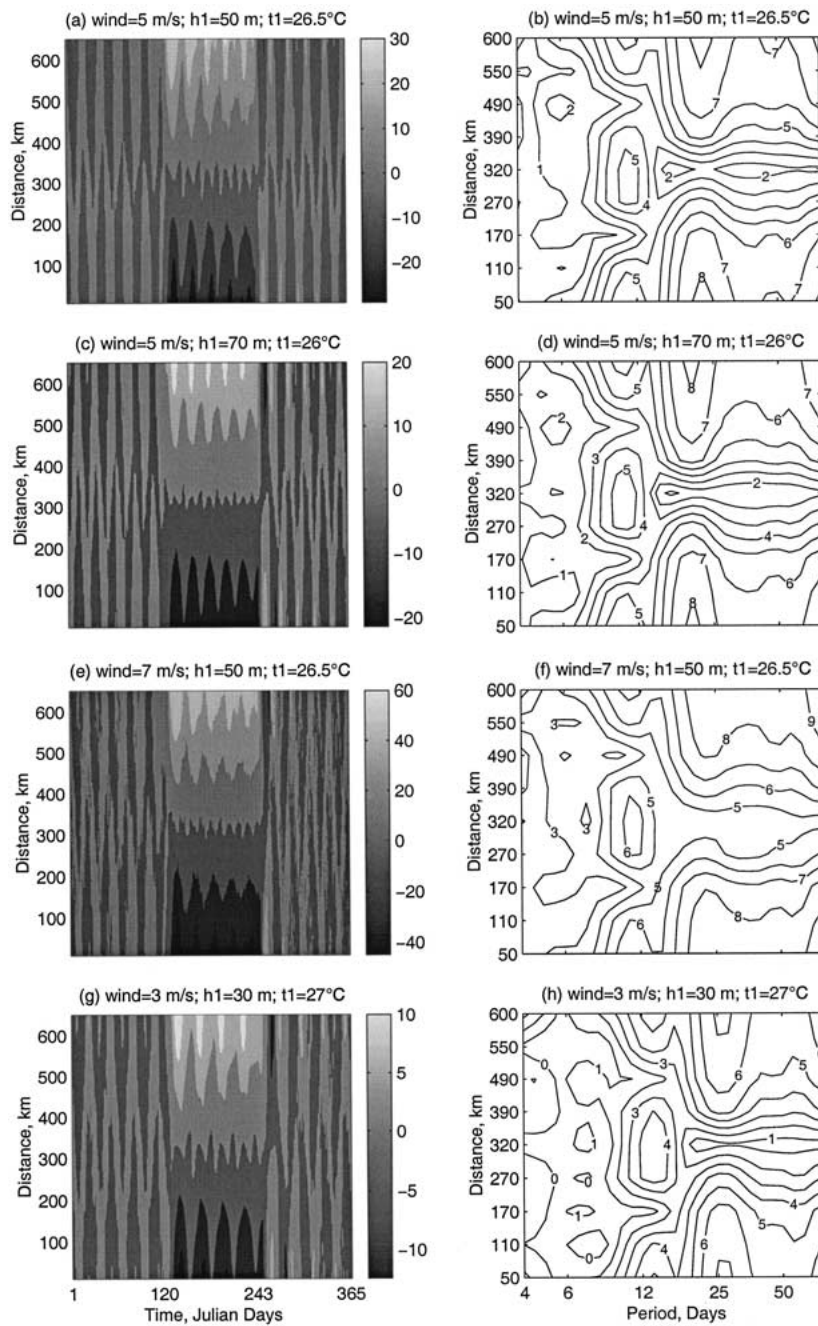
Figure 7. Same as Figure 6 for various model parameters. Temperature is increased by 0.5 °C in (a,b), the thermocline depth is increased in (c,d), wind and temperature are increased in (e,f) and (g,h) represents high temperatures, lower winds and shallower thermocline.

Table I. The summary of the sensivity of thermocline oscillations to model parameters.

Model parameter	Amplitude	Period
Wind stress ↑	↑	—
Stratification ↑	↓	↓
Thermocline depth ↑	↓	↓

surface as the wind forcing is increased to 7 ms^{-1}. For this set of parameters the model utilises the outcrop control algorithm. Increasing all the three parameters, decreases the period and increases the amplitude of oscillations.

We also tried to test the effect of high temperatures associated with warming events, such as ENSO, which decrease the thermocline depth [5]. Warm years seem to be characterised by decreased dry season winds. This combination of model parameters resulted in decreased amplitude and increased period of oscillations (Figures 7g, h). Table 1 summarises the sensitivity of thermocline oscillations to various model parameters. These tests imply that the lake is vulnerable to changing atmospheric conditions.

7. Discussion and Conclusions

This paper presented an analysis of the wind-induced thermocline oscillations in Lake Tanganyika using observations and a non-linear reduced-gravity model. Since it is difficult to perform measurements in the lake, the numerical model is adopted as a means to be able to simulate the actual conditions. For this reason we used constant winds for the dry season and compared the control run simulations with the only continous observations from the lake available to us for this purpose. The control run simulated the oscillations amplitude and period well. In the model the strong and almost continuous wind forcing in the four months of the dry season gives rise to the internal oscillations with periods and amplitude of oscillations similar to observations. Further sensitivity tests were performed to study the oscillations in the lake for other atmospheric conditions and thus, are likewise considered to represent the actual oscillations well. The data for comparing these tests is not available so far.

WT of the temperature data collected by buoy moored near Mpulungu reveal the presence of internal waves with peaks at 22 and 33 days down to the depth of 250 m, being prominent in the dry and wet season, respectively. Oscillations of 22 days were observed up to the depth of 300 m. The 12 day peak being present near the surface, while the rest of the peaks being more prominent around 30 m depth. Similar peaks are also revealed by the spectra of wind speed near the surface. The WT spectra also presented the semidiurnal, diurnal, synoptic and intraseasonal

peaks. Model simulations of the downward displacement of the thermocline exhibited oscillations of a fundamental mode of around 24 day and amplitude $\pm$ 30 m. Secondary modes of around 6 and 12 days have also been simulated by the model. The model simulations are qualitatively in agreement with the observations near Mpulungu.

The sensitivity of the simulated thermocline motions to the model parameters and forcing is also examined in detail. Weak winds yield a weak upwelling where the thermocline does not break to the surface. Warmer atmospheric conditions with weaker winds and shallow thermocline depth, restricts the upwelling of nutrient rich bottom water and therefore, the resulting phytoplankton bloom and fish production could be expected to be suppressed. Development of a three-dimensional numerical model of the lake is on its way, which will be coupled to an ecology model. The coupling of the two models will help in the better understanding of the primary production in the lake and their link to wind forcings and the temperature variation at seasonal and synoptic scales.

Acknowledgements

References

1. Coulter, G.W. and Spigel, R.H.: 1991, In: G.W. Coulter (ed.), *Lake Tanganyika and its Life*, pp. 49–75, Oxford University Press, London.
2. Wu, J.: 1975, Wind-induced drift currents, *J. Fluid Mech.*, **68**, 49–70.
3. Plisnier, P.-D. and Coenen, E.G.: 2001, Pulsed and dampened annual limnological fluctuations in Lake Tanganyika, M. Munawar and R.E. Hecky (eds.), *The Great Lakes of the World*, pp. 83–96, Backhuys Publishers, The Netherlands.
4. Wetzel, R.G.: 2001, *Limnology – Lake and River Ecosystems*, third edition, Academic Press.
5. Plisnier, P.-D.: 1998, Lake Tanganyika: Recent climate changes and teleconnections with ENSO, In: G. Demarée, J. Alexandre and M. De Dapper (eds.), *Proceedings of International Conference of Tropical Climatology, Meteorology and Hydrology 2000*, pp. 228–250.
6. Plisnier, P.-D., Serneels, S. and Lambin, E.F.: 2000, Impact of ENSO on East Africa ecosystems: a multivariate analysis based on climate and remote sensing data, *Glob. Ecol. Biogeogr.* **9**, 481–497.
7. Talling, J.F.: 1966, The annual cycle of stratification and phytoplankton growth in Lake victoria (East africa), *Intern. Rev. Gesampt. Hydrobiol. Hydrogr.* **51**, 545–621.
8. Eccles, D.H.: 1974, An outline of the physical limnology of Lake Malawi (Lake Nyasa), *Limnol. Oceanogr.* **19**, 730–742.
9. Newell, B.S.: 1960, The hydrology of Lake victoria. *Hydrobiologia* **15**, 363–383.

10. Meyers, S.D., Kelley, B.G. and O'Brien, J.J.: 1993, An introduction to wavelet analysis in oceanography and meteorology: With application to the dispersion of yanai waves, *Mon. Wea. Rev.* **121**, 2858–2866.

11. Busalacchi, A.J. and O'Brien, J.J.: 1980, The seasonal variability in a model of the tropic Pacific, *J. Phys. Oceanogr.* **10**, 1929–1951.

12. Busalacchi, A.J. and O'Brien, J.J.: 1981, Interannual variability of the equatorial Pacific in the 1960's, *J. Geophys. Res.* **86**, 10,901–10,907.

13. Luthar, M. and O'Brien, J.J.: 1985, A model of the seasonal circulation in the Arabian Sea forced by observed winds, *Progr. Oceanogr.* **14**, 353–385.

14. Woodberry, K.E., Luthar, M.E. and O'Brien, J.J.: 1989, The wind-driven seasonal circulation in the southern tropical Indian Ocean, *J. Geophys. Res.* **94**, 17,985–18,002.

15. Young, B. De, Otterson, T. and Greatbatch, R.J.: 1993, The local and nonlocal response of Conception Bay to wind forcing, *J. Phys. Oceanogr.* **23**, 2636–2649.

16. Inoue, M. and Welsh, S.E.: 1993, Modelling seasonal variability in the wind-driven upper-layer circulation in the Indo-Pacific region, *J. Phys. Oceanogr.* **23**, 1411–1436.

17. Handoh, I.C. and Bigg, G.R.: 2001, Use of a reduced-gravity model to evaluate present and past primary productivity in the tropical open ocean, *Limnol. Oceanogr.* **46**, 1632–1641.

18. Balzano, A.: 1998, Evaluation of methods for numerical simulation of wetting and drying in shallow water flow models, *Coast. Engin.* **34**, 83–107.